



SCIENTIFIC REPORTS



OPEN

Fungus-derived hydroxyl radicals kill hepatic cells by enhancing nuclear transglutaminase

Ronak Shrestha^{1,2}, Rajan Shrestha¹, Xian-Yang Qin¹, Ting-Fang Kuo¹, Yugo Oshima ³, Shun Iwatani², Ryutaro Teraoka¹, Keisuke Fujii², Mitsuko Hara¹, Mengqian Li¹, Azusa Takahashi-Nakaguchi⁴, Hiroji Chibana⁴, Jun Lu⁵, Muye Cai⁵, Susumu Kajiwara² & Soichi Kojima ¹

We previously reported the importance of induced nuclear transglutaminase (TG) 2 activity, which results in hepatic cell death, in ethanol-induced liver injury. Here, we show that co-incubation of either human hepatic cells or mouse primary hepatocytes derived from wild-type but not TG2^{-/-} mice with pathogenic fungi *Candida albicans* and *C. glabrata*, but not baker's yeast *Saccharomyces cerevisiae*, induced cell death in host cells by enhancing cellular, particularly nuclear, TG activity. Further pharmacological and genetic approaches demonstrated that this phenomenon was mediated partly by the production of reactive oxygen species (ROS) such as hydroxyl radicals, as detected by a fluorescent probe and electron spin resonance. A ROS scavenger, N-acetyl cysteine, blocked enhanced TG activity primarily in the nuclei and inhibited cell death. In contrast, deletion of *C. glabrata nox-1*, which encodes a ROS-generating enzyme, resulted in a strain that failed to induce the same phenomena. A similar induction of hepatic ROS and TG activities was observed in *C. albicans*-infected mice. An antioxidant corn peptide fraction inhibited these phenomena in hepatic cells. These results address the impact of ROS-generating pathogens in inducing nuclear TG2-related liver injuries, which provides novel therapeutic targets for preventing and curing alcoholic liver disease.

The liver acts as the first barrier to the spread of bacteria as well as fungi present in intestine. There is growing evidence on the important role of gut microbiota such as the bacteria-liver interaction in the pathogenesis of alcoholic steatohepatitis (ASH) and non-alcoholic steatohepatitis (NASH)¹⁻⁴. However, the role of intestinal fungi still remains much unclear. Recently, sequencing of the fecal microbiome showed overgrowth of *Candida albicans* (*C. albicans*) in ASH patients⁵. Among the different *Candida* species, the opportunistic pathogens *C. albicans* and *C. glabrata* rank as the two most common species in the human digestive tract and are responsible for 65–75% of systemic candidiasis, which has a high morbidity and mortality rate^{6,7}. In immunocompromised cases, these fungi might invade gastrointestinal mucosa to reach the liver and cause severe fungal infections^{8,9}. Hepatic *Candida* infection is the most commonly recognized complication in patients with acute leukaemia and other haematological malignancies that prominently involve the liver⁹. A prospective study performed 25 years ago reported that fungal infection was present in 32% of patients with acute liver failure and that *Candida* species were the principle fungus present, although the underlying molecular mechanisms of these infections remain to be elucidated¹⁰.

Transglutaminase 2 (TG2, EC 2.3.2.13) is the most ubiquitously expressed Ca²⁺-dependent protein-crosslinking enzyme implicated in the regulation of cell growth, differentiation and apoptosis¹¹. Previously, we addressed the role of induced cellular TG activity in hepatic cell death during the pathogenesis of both alcoholic and non-alcoholic steatohepatitis via crosslinking and inactivation of the general transcription factor Sp1, which resulted in the decreased expression of growth factor receptors essential to cell survival^{12,13}.

¹Micro-Signaling Regulation Technology Unit, RIKEN Center for Life Science Technologies, Wako, Saitama, Japan.

²School of Life Science and Technology, Tokyo Institute of Technology, Yokohama, Kanagawa, Japan. ³Condensed Molecular Materials Laboratory, RIKEN, Wako, Saitama, Japan. ⁴Medical Mycology Research Center, Chiba University, Chiba, Chiba, Japan. ⁵China National Research Institute of Food and Fermentation Industries, Beijing, China. Ronak Shrestha, Rajan Shrestha and Xian-Yang Qin contributed equally to this work. Correspondence and requests for materials should be addressed to S.K. (email: skajiwara@bio.titech.ac.jp) or S.K. (email: skojima@riken.jp)

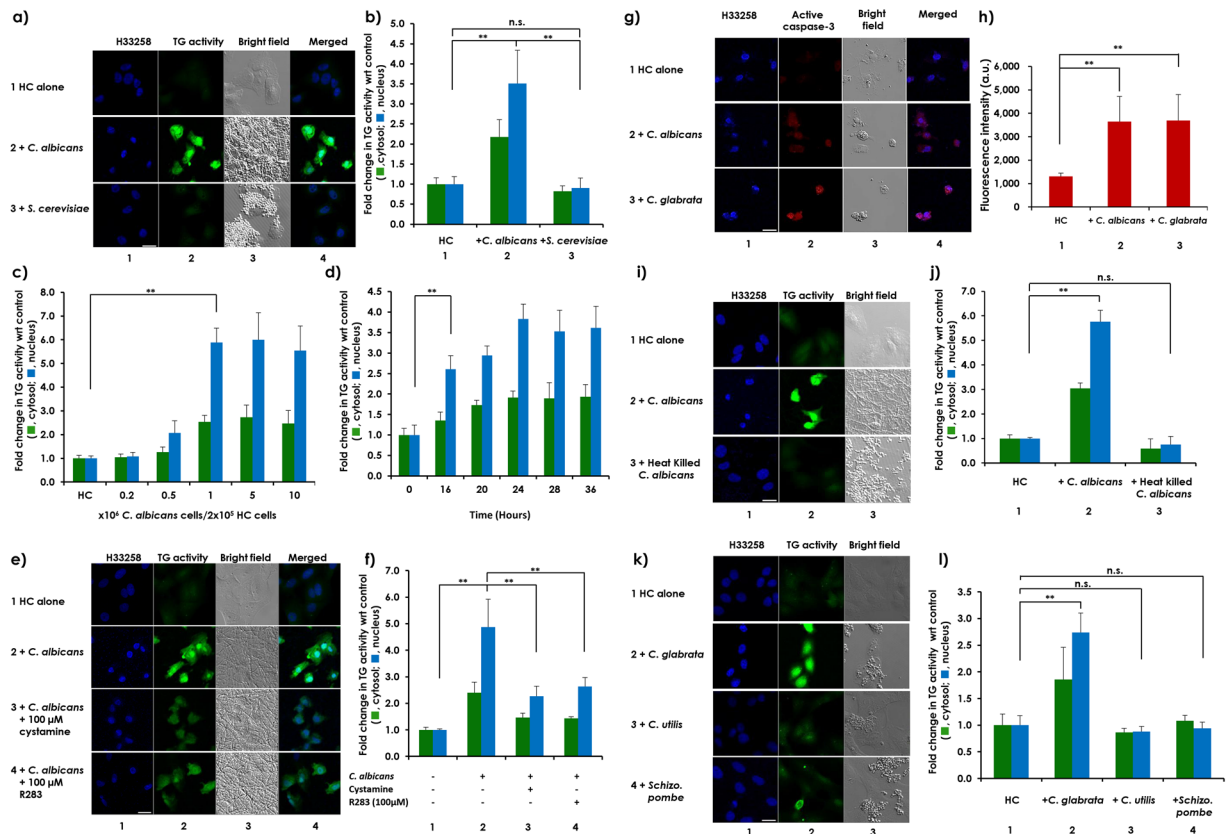


Figure 1. Cellular TG activity in HC cells increased, especially in the nucleus, upon co-incubation with pathogenic fungi. HC cells were seeded at 2×10^5 cells per well in a 6-well plate and incubated overnight. After adding 5-BAPA, the cells were incubated (a) alone (row 1) or were co-incubated with 2.5×10^6 *C. albicans* cells (row 2) or *S. cerevisiae* cells (row 3) for 24 hours; (c) with different doses of *C. albicans* cells for 24 hours; (d) with 5×10^6 *C. albicans* cells in the absence (row 2) and presence of 100 μ M of TG2 inhibitors, cystamine (row 3) or R283 (row 4) for 24 hours; (g) alone (row 1) or were co-incubated with either 5×10^6 *C. albicans* cells (row 2) or the same number of *C. glabrata* cells (row 3) in an insert cup with a 0.4- μ m pore size; (i) alone (row 1) or were co-incubated with living 5×10^6 (row 2) or heat-killed 5×10^9 (row 3) *C. albicans* cells for 24 hours; or (k) alone (row 1) or were co-incubated with living 5×10^6 *C. glabrata* (row 2), *C. utilis* (row 3) and *Schizo. pombe* cells (row 4) for 24 hours. Scale bars = 20 μ m. Representative images from at least 3 fields from 3 independent experiments are shown for (a, e, i and k) and from at least 3 fields from a single experiment for (g). Fluorescence intensities from TRITC in both the cytoplasm and nucleus of panels (b, c, d, f and j) were quantitated using ZEN 2011 software, and relative TG activity levels in both locations are presented in bar graphs, with the levels from HC cells incubated alone (panels b, c, f, h and j) or at time 0 (d) used as the controls (mean \pm SD, n = 3). Fluorescence intensities from Alexa 488 signal from panel (h) were quantitated using ZEN 2011 software, and the mean \pm SD are presented in bar graphs after subtraction of background intensities. Asterisks represent statistical significance.

Intracellular reactive oxygen species (ROS) have been reported to activate TG2 in different cell types^{14–16}. Intriguingly, TG2 exhibits multiple additional functions in the regulation of cell growth and death depending upon the cell type and stimuli¹⁷. In dying cells, intracellular ROS enhances TG2 activation, which facilitates Bax translocation to the mitochondria. Thus, the release of cytochrome *c* and apoptosis-inducing factors from the mitochondria can induce both caspase-dependent and caspase-independent apoptotic cell death, respectively¹⁸.

Here, by investigating the cellular activity of TG2 in a human hepatic cell line (HC cells) and mouse primary hepatocytes following co-incubation with *Candida* species, we explored the hypothesis that these fungi might induce the nuclear activity of TG2 in hepatic cells. We show that ROS-producing fungi such as *C. albicans* and *C. glabrata* are associated with enhanced cellular activity, particularly nuclear TG activity, in hepatic cells, which led to apoptosis. A similar phenomenon was reproduced in the livers of mice injected with *Candida* species. We found that co-incubation of hepatic cells with opportunistic fungi, such as *C. albicans* and *C. glabrata*, but not edible yeasts, such as *Saccharomyces cerevisiae*, induces hepatic cell death by enhancing TG activity, at least in part through the production of ROS, such as hydroxyl radicals. An irreversible inhibitor of TG2, 6-diazo-5-oxo-norleucine tetrapeptide (ZDON)¹⁹, inhibited *C. albicans*-induced cell death as measured by caspase-3 activation. Further pharmacological and genetic approaches demonstrated that this phenomenon was mediated partly by intracellular ROS. A specific inhibitor of ROS, N-acetyl cysteine (NAC)¹⁴, inhibited the induction of cellular TG activity and cell death. Deletion of an NADPH oxidase gene (*NOX1*) in *C. glabrata*, which encodes a ROS-generating enzyme, failed to induce the

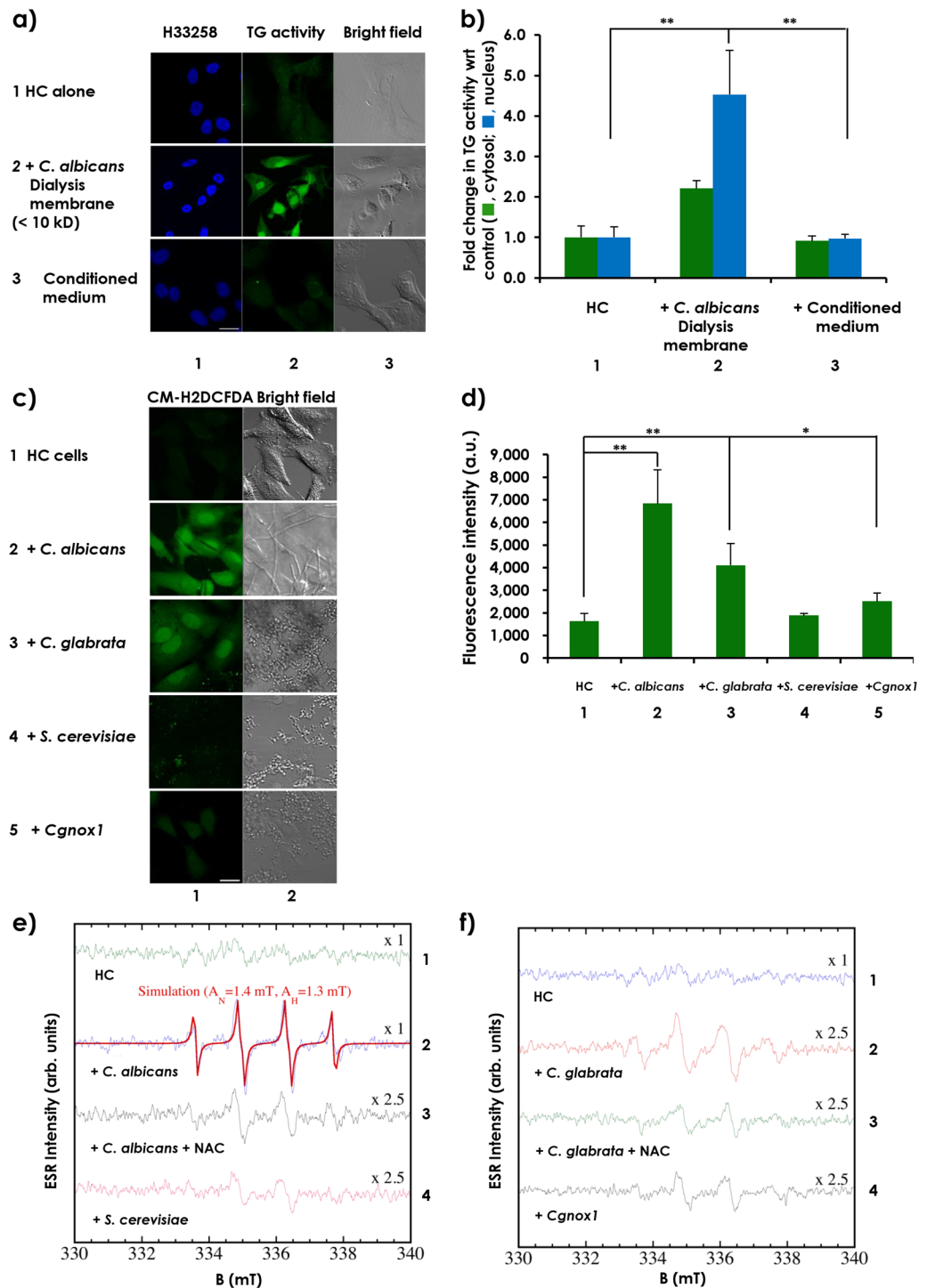


Figure 2. Levels of ROS in HC cell were increased following co-incubation with pathogenic *Candida* species. HC cells were seeded at 2×10^5 cells per well on a 35-mm glass-based dish or round cover slips plated in 6-well plates and were incubated overnight. **(a)** After adding 5-BAPA, the cells were incubated alone (row 1) or were co-incubated with 5×10^6 *C. albicans* cells grown in a transwell separated by a dialysis membrane (row 2) or with the conditioned medium prepared from *C. albicans* cultures following a 24-hour incubation (row 3). Representative images from at least 3 fields from 3 independent experiments are shown. **(b)** Fluorescence intensities of TRITC in both the cytoplasm and nucleus were quantitated using ZEN 2011 software, and the relative TG activity levels are presented in bar graphs with the levels from the HC cells incubated alone as the control (mean \pm SD, $n = 3$). **(c)** Cells were incubated alone (row 1) or were co-incubated for 8 hours with the different fungal strains, including *C. albicans* (row 2), *C. glabrata* (row 3), *S. cerevisiae* (row 4), and the *CgNOX1* gene-targeted mutant of *C. glabrata* (row 5), with $5 \mu\text{M}$ CM-H2DCFDA. Scale bars = $20 \mu\text{m}$. **(d)** Fluorescence intensities from reacted CM-H2DCFDA were quantitated using ZEN 2011 software and are represented in bar graphs (mean \pm SD, $n = 3$). A $100\text{-}\mu\text{L}$ test mixture was prepared containing $40 \mu\text{L}$ DPTA, $10 \mu\text{L}$ BMPO and **(e)** $50 \mu\text{L}$ of culture medium from the HC cells (spectrum 1) or HC cells co-incubated with *C. albicans* in the

absence (spectrum 2) or presence (spectrum 3) of NAC or *S. cerevisiae* (spectrum 4) cultivated for 8 hours or with (f) 50 μ L of culture medium from HC cells (spectrum 1), or HC cells were co-incubated with *C. glabrata* in the absence (spectrum 2) or presence (spectrum 3) of NAC or *Cgnox1* (spectrum 4) for 8 hours. The mixture was transferred to a quartz flat cell and set inside the cavity of the ESR spectrometer and analyzed using the data analyzer connected to the ESR spectrometer.

same phenomena. These findings provide additional mechanistic insights into the exacerbation of liver (tissue) injury by pathogenic fungi and the importance of ROS removal for liver protection.

Results

Co-incubation of *C. albicans* or *C. glabrata* with HC cells increased cellular TG and caspase-3 activity levels in HC cells. Co-incubation of a hepatic cell line (HC) with *C. albicans*, but not with *S. cerevisiae*, enhanced the cellular incorporation of 5-(biotinamido)pentylamine (5-BAPA), a TG substrate (Fig. 1a and b, compare rows or columns 1 with 2 and 3, respectively). Maximum 2.5- and 6-fold increases in TG activity were observed in cytosolic and nuclear regions, respectively, in a dose- and time-dependent manner, reaching a plateau after the co-incubating of 2×10^5 HC cells with 5×10^6 *C. albicans* cells for 24 hours (Fig. 1c and d). Both cystamine (a broad TG inhibitor) and R283²⁰ (a site-directed specific TG inhibitor) significantly inhibited *C. albicans*' induction of cellular TG activity in HC cells (Fig. 1e and f, rows or columns 3 and 4, respectively), suggesting that more than 60% of the detected TG activity in HC cells was induced by *C. albicans*. TG2 mRNA levels were also enhanced in HC cells upon co-incubation with *C. albicans* for 8 hours (Fig. S1a). In EGFP-TG2-overexpressing HC cells, co-incubation with *C. albicans* for 24 hours caused a nuclear accumulation of the overexpressed TG2 (Fig. S1b and S1c). Although no significant decrease in the number of HC cells was observed after co-incubation for 24 hours, the cells became smaller in size. However, further co-incubation to 48 hours resulted in caspase-3 activation and cell death (Fig. 1g and h, compare rows and columns 1 with 2). In contrast, heat-killed *C. albicans* lost its capacity to increase TG activity in HC cells (Fig. 1i and j, compare rows or columns 1 with 3). Another pathogenic species, *C. glabrata*, but not the edible species *C. utilis* or the fission yeast *Schizosaccharomyces pombe*, showed a capacity to induce cellular TG activity similar to that of *C. albicans* (Fig. 1k and l, compare rows or columns 1 with 2, 3 and 4, and Fig. 1g and h, compare rows and columns 1 with 3). Next, pharmacological approaches were employed to determine whether inhibition of TG2 activation might affect fungus-induced hepatic cell death. An irreversible inhibitor of TG2, ZDON, significantly inhibited *C. albicans*-induced cell death as measured by caspase-3 activation in a human hepatocarcinoma functional liver cell-7 (FLC-7) cell line (Fig. S2). In addition, a nuclear TG2 inhibitor, phenosafranine, which inhibits nuclear localization of TG2 without affecting the transaminase activity itself²¹, also significantly inhibited *C. albicans*-induced caspase-3 activation in FLC-7 cells (Fig. S2), suggesting that nuclear TG2 activity is involved in *C. albicans*-induced hepatic cell death. Furthermore, the effect of *C. albicans* infection was compared between TG2 wild-type (TG2^{+/+}) and knockout (TG2^{-/-}) mice. Infection with *C. albicans* administered via tail vein induced death of the animals in a dose-dependent manner (Fig. S3a). Although both showed time-dependent decreases in body weight after infection with a non-lethal dose of 4×10^5 *C. albicans*, a significantly attenuated body weight loss was observed in TG2^{-/-} mice compared to TG2^{+/+} mice (Fig. S3b and S3c).

Co-incubation with pathogenic *Candida* species increased levels of ROS in HC cells. Because induction of cellular TG activity required co-incubation with living pathogenic fungi, we wanted to estimate the molecular size of the mediator produced from fungi. To this end, HC cells were co-incubated with *C. albicans* plated in a dialysis membrane (cutoff <10 kDa). Increased cellular TG activity was observed in HC cells treated with the fungus in transwell plates (Fig. 2a and b, compare rows or columns 1 with 2) but not in HC cells treated with the fungus-conditioned media (Fig. 2a and b, compare rows or columns 1 with 3). This finding suggests that a certain soluble factor(s), which might be very unstable in nature, was secreted into the culture medium by *C. albicans* and caused increased cellular TG activity. Suspecting that unstable substances, such as ROS, might act as promising mediators, and ROS generation was measured using the fluorescent probe 5–6-chloromethyl-2', 7'-dichlorodihydrofluorescein diacetate (CM-H2DCFDA)²² (Fig. 2c and d). Significantly higher levels of ROS were produced by both *C. albicans* (row and column 2) and *C. glabrata* (row and column 3) than by HC cells alone (row and column 1) or by *S. cerevisiae* (row and column 4). The capacities of *C. albicans* and *C. glabrata* to produce higher levels of ROS may characterize them as pathogenic fungi. In *C. glabrata*, the only known gene (CAGL0K05863g) homologous to the genuine NADPH oxidase Yno1p/Aim14p of *S. cerevisiae*²³ was identified (and named *CgNOX1*) and was determined to be responsible for the generation of superoxide from oxygen. We prepared *Cgnox1*-disruption mutants and confirmed the decrease in ROS generation (row and column 5).

To determine the ROS species, electron spin resonance (ESR) analyses were performed, and high levels of hydroxyl radicals (\cdot OH) were identified in freshly harvested HC cells co-cultured with conditioned medium from *C. albicans* (Fig. 2e) and *C. glabrata* (Fig. 2f), but not in the medium of the *Cgnox1* mutants, relative to the HC cell-conditioned medium (Fig. 2e and f). The order of the \cdot OH spectrum intensities was *C. albicans* > *C. glabrata* > *S. cerevisiae*, with an approximate ratio of 10:3:1, respectively (Fig. 2e and f). The \cdot OH spectrum intensity of *Cgnox1* was also quite small (almost the same as that of *S. cerevisiae*). Treatment of HC cells and *C. albicans*/*C. glabrata* co-cultures with NAC also showed spectra similar to that of \cdot OH but with different hyperfine parameters ($A_H = 1.5$ mT $A_N = 1.4$ mT). We speculate that this might be an extrinsic effect due to the interactions of NAC, \cdot OH and 5-tert-butoxycarbonyl-5-methyl-1-pyrroline-N-oxide (BMPO). These results indicate that certain levels of exogenous ROS trigger the induction of nuclear TG in adjacent hepatic cells.

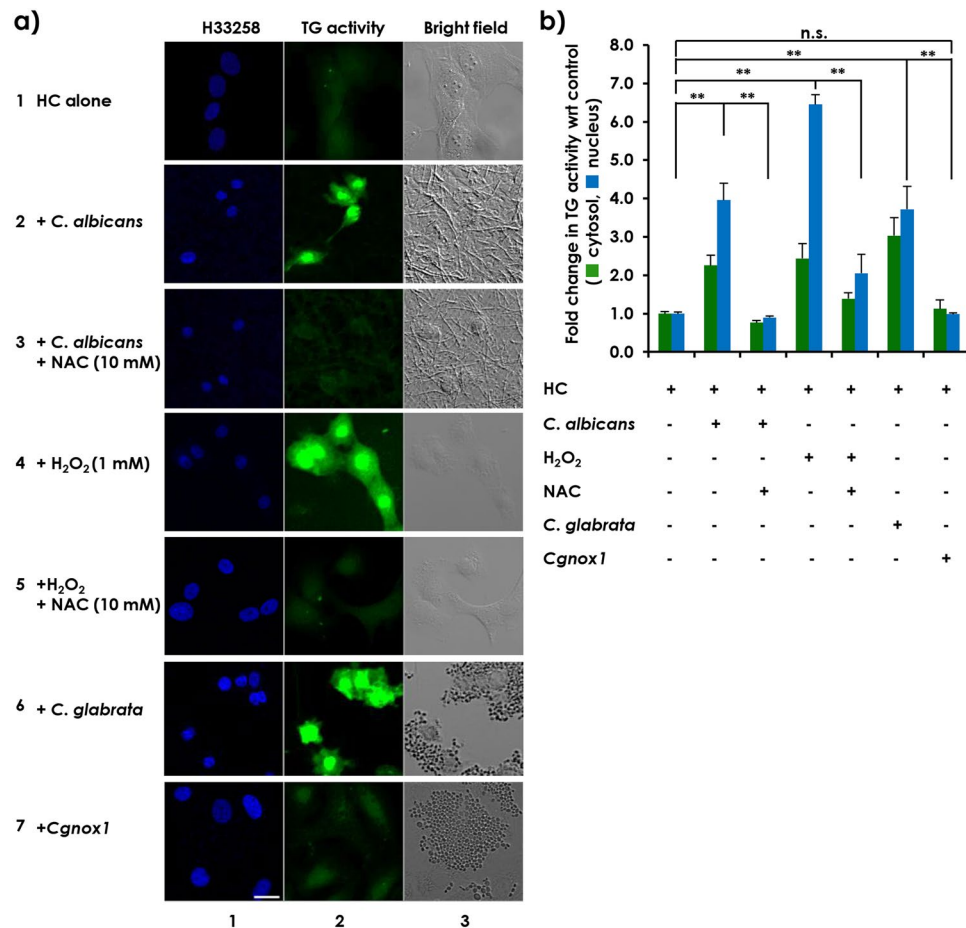


Figure 3. ROS produced by *C. albicans* induced cellular TG activity in HC cells. HC cells were seeded at 2×10^5 cells per well in a 35-mm glass-based dish or on round cover slips plated in 6-well plates and incubated overnight as previously described. (a) After adding 5-BAPA, the HC cells were incubated alone (row 1) or were co-incubated for 24 hours with 5×10^6 *C. albicans* cells in the absence (row 2) or presence (row 3) of 10 mM NAC, with 1 mM H₂O₂ in the absence (row 4) or presence (row 5) of 10 mM NAC, or with 5×10^6 *C. glabrata* cells (row 6) or *Cgnox1*-mutant cells (row 7). The cells were fixed and stained with streptavidin-TRITC and H33258 dye. Both the blue fluorescence signals from H33258-stained nuclei (column 1) and the green fluorescence signals representing TG activity (column 2) were detected using a confocal microscope. Images taken under the bright field (column 3) are also shown. Scale bars = 20 μ m. Representative images from at least 3 fields from 3 independent experiments are shown. (b) Fluorescence intensities from TRITC in both the cytoplasm and nucleus were quantitated using ZEN 2011 software, and the relative TG activity levels in both locations are represented in bar graphs, with the level from HC cells incubated alone used as the control (mean \pm SD, n = 3).

Candida species-derived ROS-induced enhancement of cellular and, to a greater extent, nuclear TG activity in HC cells. To explore whether fungus-derived ROS might mediate induction of cellular TG activity in HC cells, cells were co-incubated with *C. albicans* in the presence and absence of NAC, an inhibitor of ROS¹⁴. Treatment of the co-cultures of *C. albicans* and HC cells with NAC completely blocked the enhanced cytosolic and nuclear TG activities in HC cells (Fig. 3a and b, compare rows or columns 2 with 3). These results suggest that ROS might mediate the enhancement of cellular and, to a greater extent nuclear, TG activity in HC cells. This hypothesis was verified by both gain- and loss-of-function experiments. First, to examine the capacity of ROS to induce increased TG activity, HC cells were treated with H₂O₂ in the presence or absence of NAC. Similar to HC cells co-incubated with *C. albicans*, externally added H₂O₂ mimicked an increase in cellular TG activity in HC cells, which was blocked by NAC (Fig. 3a and b, compare rows or columns 4 with 5). However, HC cells co-incubated with the *Cgnox1* mutant failed to increase TG activity (Fig. 3a and b, compare row or column 6 with 7). These results suggest that the ROS produced during co-incubation of HC cells with *C. albicans* and *C. glabrata* in the proximity of HC cells worked as a mediator(s) to increase cellular TG activity in HC cells.

This possibility gave rise to another intriguing question of whether naturally produced antioxidants derived from food could be inhibitors of ROS production and applied to prevent and manage pathogenic fungal infection-induced TG activity²⁴. Therefore, we screened an antioxidant corn peptide fraction (CP), which inhibited *C. albicans*-induced TG activity in HC cells (Fig. 4a and c) concomitantly with an inhibition of *C.*

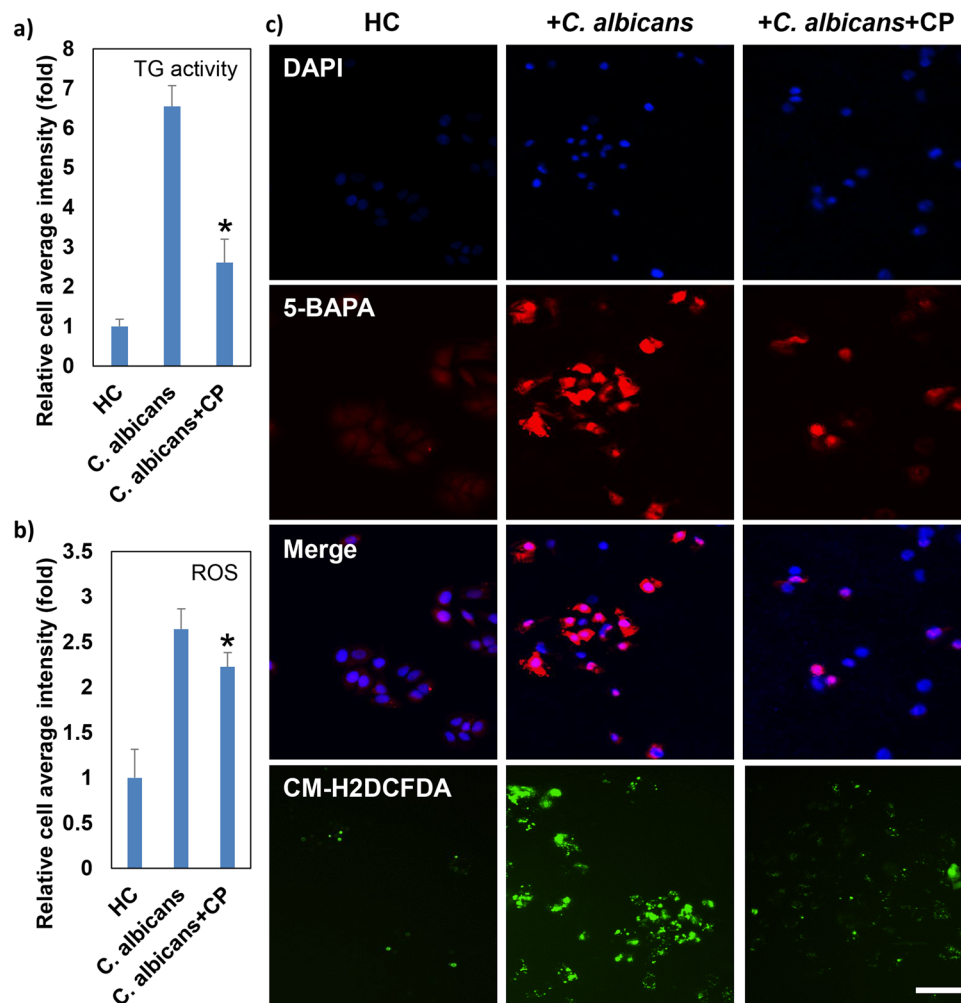


Figure 4. Antioxidant corn peptide fraction inhibits *C. albicans*-induced TG activity in HC cells. HC cells were seeded at 1×10^4 cells per well in a 96-well plate and were incubated overnight as previously described. Cells were incubated alone (HC) or were co-incubated with 1×10^6 *C. albicans* cells (*C. albicans*) in the presence of $100 \mu\text{g/mL}$ corn peptide fraction (*C. albicans* + CP). (a) TG activity in the cells was detected by 5-BAPA incorporation, as previously described. After 24 hours, cells were fixed and stained with streptavidin-TRITC and 4',6-diamidino-2-phenylindole (DAPI) dye. Both the blue fluorescence signals from DAPI-stained nuclei and the red fluorescence signals representing TG activity were detected with the ImageXpress^{MICRO} High Content Screening System, and morphological analysis was performed using MetaXpress Image Analysis software. (b) After 24 hours, cells were incubated with $5 \mu\text{M}$ CM-H2DCFDA for ROS detection. Green fluorescence signals from CM-H2DCFDA representing ROS were observed with the ImageXpress^{MICRO} High Content Screening System (Molecular Devices, Sunnyvale, CA, USA), and morphological analysis was performed using MetaXpress Image Analysis software (Molecular Devices). The representative quantitative data are presented as the mean \pm SD of at least three replicates from two independent experiments. (c) Representative fluorescence images from at least 4 fields from more than three samples of two independent experiments. Scale bar = $50 \mu\text{m}$.

albicans-induced ROS generation in HC cells (Fig. 4b and c). Furthermore, these results also demonstrated that in combination with high content screening technology, the *in vitro* co-culture system of pathogenic fungi and hepatic cells presented in this study provided a unique and powerful tool for the discovery of nuclear TG inhibitors.

Candida species-derived ROS-induced caspase-3 activity following increased cellular TG activity in HC cells and mouse primary hepatocytes. Next, to explore the role of ROS in caspase-3 activation, HC cells were incubated with pathogenic fungi. Enhanced cellular TG activity and caspase-3 activation were observed and were attenuated by NAC (Fig. 5a and b, compare row or column 2 with 3). Primary hepatocytes from TG2^{+/+} and TG2^{-/-} mice were treated with different strains of fungi (Fig. 5c and d). Increased cellular TG and caspase-3 activity levels were observed following co-culturing *C. albicans* or *C. glabrata* with TG2^{+/+} hepatocytes (compare rows 1 with 3 and 5, respectively) but not with TG2^{-/-} hepatocytes (compare rows 2 with 4 and 6, respectively) or TG2^{+/+} hepatocytes treated with *Cgnox1* (row 9), *C. utilis* (row 10) or *S. cerevisiae* (row 11). The increased TG activity and caspase-3 activation were attenuated by NAC (compare rows 3 with 7 and 5 with 8),

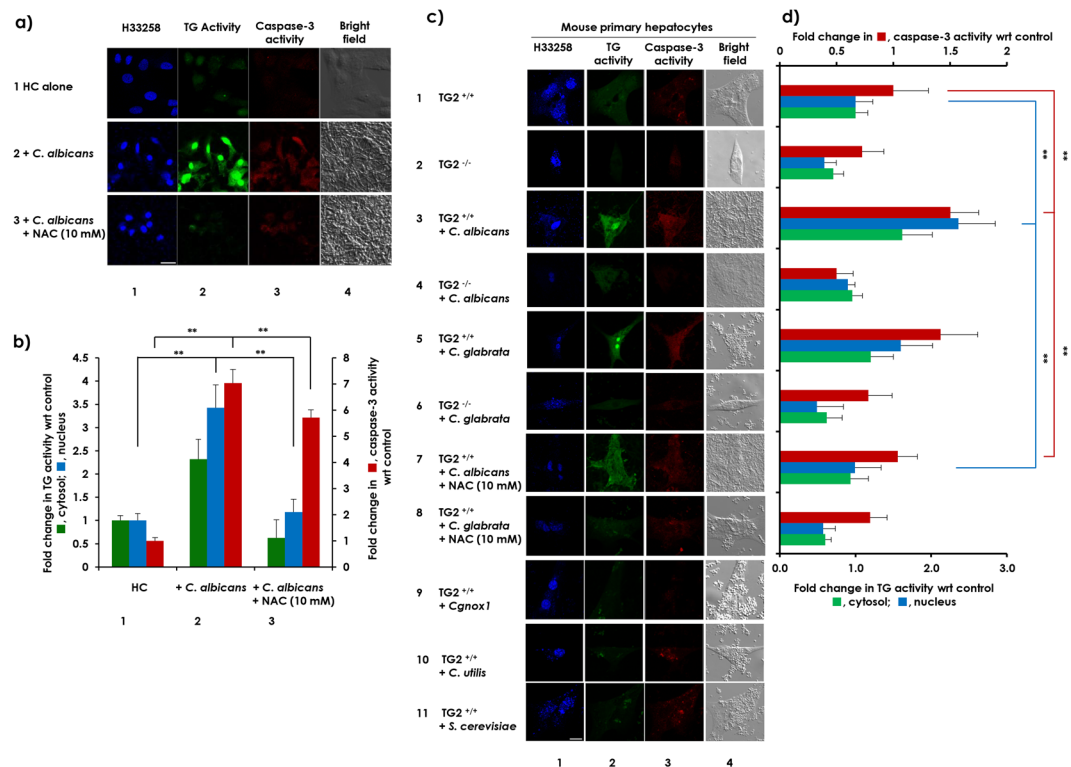


Figure 5. ROS derived from *C. albicans* and *C. glabrata* induced cell death in HC cells and mouse primary hepatocytes. **(a)** HC cells were seeded at 2×10^5 cells per well in a 6-well plate and were incubated overnight and then treated with 5-BAPA and were incubated alone (row 1) or were co-incubated with 5×10^6 *C. albicans* cells (row 2) in the presence of 10 mM NAC (row 3). **(c)** Primary hepatocytes isolated from livers of TG^{-/-} mice and their TG^{+/+} littermates were seeded at 5×10^5 cells per well in a 6-well plate and incubated overnight. The next day, the cells were treated with 5-BAPA and incubated alone (rows 1 and 2) or were co-incubated with 5×10^6 *C. albicans* cells (rows 3 and 4) in the presence of 10 mM NAC (row 7) or with the same number of *C. glabrata* cells (rows 5 and 6) in the presence of 10 mM NAC (row 8), *Cgnox1* (row 9), *C. utilis* (row 10), and *S. cerevisiae* (row 11). The blue fluorescence from H33258 dye (column 1) was observed along with the green fluorescence signals from TRITC staining 5-BAPA representing TG activity (column 2) and red fluorescence from Alexa 488 representing caspase-3 activity (column 3) using a confocal microscope. An image taken under bright field (column 4) is also shown. Scale bar = 20 μ m. Representative images from at least 3 fields from a single experiment are shown. **(b and d)**. Fluorescence intensities from TRITC in both the cytoplasm and nucleus along with fluorescence intensities from Alexa 488 were quantitated using ZEN 2011 software, and after subtraction of background intensities, the relative TG and caspase-3 activity levels are represented in bar graphs, with the levels from HC cells or TG^{+/+} primary hepatocytes incubated alone as the control (mean \pm SD, n = 3).

indicating that fungi-derived ROS increases cellular TG activity, especially TG2, and increases caspase-3 activation, leading to cell apoptosis.

In vivo *C. albicans* infection-induced ROS production and TG activity in mouse livers. Finally, to evaluate whether injection of pathogenic fungi can also induce *in vivo* hepatic TG activity, mice were infected with *C. albicans* administered via the tail vein (Fig. S4a). Three days after injection, a significant decrease in body weight was observed in *C. albicans*-infected mice relative to the control mice (Fig. S4b). Histological and fluorescence staining of the liver sections showed that there were more inflammatory cell infiltrations and higher levels of ROS in livers infected with *C. albicans* (Fig. S4c and S4d). To evaluate *in vivo* TG activity, 30 minutes prior to euthanasia, mice were injected with approximately 100 μ g/g of 5-BAPA by intraperitoneal injection. Mice were then euthanized, and sections of fresh-frozen tissue were stained with streptavidin-TRITC for immunofluorescence detection. As the results indicate, increased TG activity was observed in the periportal area in *C. albicans*-infected mouse livers, suggesting that the induction of TG activity due to pathogenic fungal infection might contribute to liver injury (Fig. S4e).

Discussion

Although the roles of the gut microbiota and bacteria-liver interactions are fairly well understood in the context of ASH and NASH¹⁻⁴, the role of intestinal fungi still remains unclear. Recently Yang *et al.* reported the induction of *C. albicans* in ASH patients⁵. Here, we demonstrated, for the first time, an association of ROS-producing fungi, such as *C. albicans* and *C. glabrata* with enhanced nuclear TG2 activity in hepatic cells leading to apoptosis,

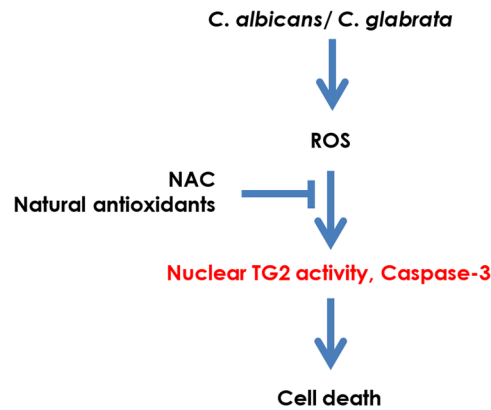


Figure 6. Schematic diagram showing the mechanism of *C. albicans*- and *C. glabrata*-induced cell death in HC cells. Both fungi produce ROS that induces cellular TG activity leading to HC cell death. NAC and natural antioxidants are effective in preventing this cell death by blocking the action of ROS.

illustrating the impact of ROS-generating pathogens in inducing or exacerbating nuclear TG2-related liver injuries, which may provide a molecular mechanism of hepatic injury observed in ASH/NASH patients.

We found that *C. albicans* and *C. glabrata* produced high levels of ROS. This ability may be characterized as one of the pathogenic factors of *C. albicans* and *C. glabrata*. This result is consistent with the findings of Schröter *et al.*²⁵, who found that *C. albicans* generates ROS and releases it extracellularly. Indeed, hydroxyl radicals were detected in the conditioned medium freshly isolated from those fungi. Reproducible enhancement of cellular TG activity by fungal ROS and exogenously added H₂O₂ were observed, while the ROS scavenger NAC blocked these effects. Furthermore, a mutation in *NOX1* in *C. glabrata*, which eliminated its capacity to produce ROS, abrogated the capacity of *C. glabrata* to enhance cellular TG activity. These results suggest that the ROS produced by *C. albicans* and *C. glabrata* in close proximity to HC cells acted as a principal mediator(s) in increasing cellular, especially nuclear, TG activity in the HC cells and, eventually, induced cell death (Fig. 5). A similar phenomenon was reproduced in *C. albicans*-infected mouse livers (Fig. S4). However, we cannot rule out the possibility that *C. albicans* and *C. glabrata* might also stimulate endogenous ROS production in HC cells. We are currently investigating the underlying molecular mechanisms of the production of high levels of ROS by *C. albicans* and *C. glabrata* and those for the ROS-induced enhancement of cellular TG activity. ROS can directly inactivate TG2²⁶. Thus far, we have observed that ROS enhances both the gene expression and nuclear localization of TG2 in HC cells.

Increased intracellular ROS production has been reported to be the principal mediator for TG2 activation in human umbilical vein endothelial cells (HUVEC) lines treated with C-peptide¹⁶, in Swiss 3T3 cell lines treated with lysophosphatidic acid (LPA) and transforming growth factor beta (TGF-β)¹⁴, and in NIH3T3 cell lines treated with arachidonic acid¹⁵. In these studies, endogenously produced ROS enhanced cellular TG activity, although the biological relevance of this enhancement was not addressed. In addition, it has been reported that *C. albicans* produces ROS under certain conditions²⁵. Combining these previous findings and the results of the current study suggests that host cell (tissue) injury by *Candida* via the ROS-mediated induction of nuclear TG2 might be a general phenomenon. Indeed, we observed a similar induction of nuclear TG2 in HEK293T cells, a human embryonic kidney cell line, upon co-incubation with *C. albicans* (data not shown). Concomitant bacterial infection with fungal infection has been previously reported^{10,27}. We are currently investigating the effect of ROS-generating bacteria on the regulation of cellular TG activity in hepatic cells.

In conclusion, in this study, we demonstrate that the pathogenic fungi *C. albicans* and *C. glabrata* increase cellular TG activity levels in hepatic cells. This increase eventually leads to cell death due to the release of ROS, which acts as a principal mediator (Fig. 6). This observation suggests that the production of high levels of ROS and the ROS-mediated induction of nuclear TG2 might be a basic feature of pathogenic fungi. ROS plays a vital role in host defense and has been involved in various pathological conditions, including cardiovascular disease²⁸, neurodegenerative diseases such as Alzheimer's disease²⁹ and Parkinson's disease³⁰, diabetes¹⁶ and renal cell carcinoma³¹. TG2 has also been associated with these diseases^{32–36}. In such situations, suitable inhibitors of exogenous ROS may serve as promising therapies for liver injury in hepatitis patients by inhibiting the enhancement of cellular TG activity.

Methods

Ethics Statement. The *in vivo* infection experiments were performed in accordance with protocols approved by the RIKEN Institutional Animal Use and Care Administrative Advisory Committee (H28-2-002(3)) and adhered to the guidelines of the Institutional Regulation for Animal Experiments and Fundamental Guidelines for Proper Conduct of Animal Experiments and Related Activities in Academic Research Institutions under the jurisdiction of the Ministry of Education, Culture, Sports, Science and Technology, Japan.

Cell culture. HC cells from a human hepatic cell line were purchased from Cell Systems (Kirkland, WA, USA) and were grown in CS-C complete medium. FLC-7 cells were kindly supplied by Dr. Matsuura (The Jikei University School of Medicine, Tokyo, Japan)³⁷. The cells were cultured at 37 °C in a humidified incubator with

5% CO₂. For the experiments, cells were plated and cultured overnight in 96-well plates or 6-well plates bearing round coverslips. The next day, the cells were incubated for 4 hours in Dulbecco's modified Eagle's medium (DMEM) supplemented with 0.2% fetal bovine serum (FBS) for serum starvation (Mediatech, Herndon, VA, USA). These cells were co-incubated with fungi in the presence of 5-BAPA (Thermo Scientific, Rockford, IL, USA) in serum-free DMEM.

Isolation of primary hepatocytes. Primary hepatocytes were isolated from the livers of male TG2^{-/-} mice and their TG2^{+/+}³⁸ littermates by collagenase digestion method as described previously³⁹; the cells were then cultured in DMEM containing 10% FBS.

Fungal strains and culture conditions. Each fungal strain (Supplemental Table S1) was grown on yeast peptone dextrose (YPD, 1% yeast extract, 2% peptone, 2% dextrose and 2% agar) agar medium. For co-incubation with HC cells and *in vivo* infection, the fungi were pre-cultured in liquid YPD medium with shaking at 160 rpm for 8 to 16 hours at 30 °C. The pre-cultures were washed twice with phosphate-buffered saline (PBS) and adjusted to the desired cell density in plates by measuring the optical density at 600 nm (OD₆₀₀) using an Ultrospec 2000 spectrophotometer (Pharmacia Biotech, Piscataway, NJ, USA). For the preparation of heat-killed *C. albicans* cells, 5 × 10⁹ cells/mL from an overnight culture were washed twice with PBS and heated in DMEM at 70 °C for 20 minutes. Heat-killing of the cells was confirmed based on the loss of growth following the incubation of heated cells on YPD agar plates for 48 hours at 30 °C. Preparation of NOX1-disrupted *C. glabrata* mutants is detailed in the Supplemental Information.

Determination of *in vitro* TG activity. HC cells were seeded on round coverslips plated in a 6-well plate (2 × 10⁵ cells) and incubated overnight at 37 °C with 5% CO₂. The next day, the cells were directly or indirectly co-incubated for 24 hours with fungi using a transwell with a 0.4-μm pore size membrane or a dialysis membrane (cutoff < 10 kDa), creating a barrier between the HC cells and the fungi. The cellular activity of TG2 was measured based on the incorporation of 0.2 mM 5-BAPA into the cells incubated in the presence of 0.1 mM aminoguanidine with and without 100 μM cystamine or R283, which are TG2 inhibitors²⁰. Some samples were also incubated with 50 μM ZDON (Zedira, Darmstadt, Germany)¹⁹ or 10 μM phenosafranine (Sigma-Aldrich Co., St. Louis, MO, USA)²¹ as TG2 inhibitors, 10 mM NAC (Sigma-Aldrich Co.) as an ROS inhibitor¹⁴, or 1 mM H₂O₂ as a positive control for producing ROS. Cells were then fixed with a 10% formaldehyde solution, permeabilized, blocked and immunostained with streptavidin-tetramethylrhodamine isothiocyanate (TRITC) (Jackson ImmunoResearch Laboratories, West Grove, PA, USA) and cleaved caspase-3 (Cell Signaling Technology, Danvers, MA, USA). The TG activity was then detected as a fluorescence signal from TRITC and analyzed with an LSM 700 laser scanning confocal microscope (Carl Zeiss, Inc., Germany) using ImageXpress^{MICRO} High Content Screening System (Molecular Devices, Sunnyvale, CA, USA). The morphological analysis was performed using MetaXpress Image Analysis software (Molecular Devices). Anti-rabbit Alexa 488 was used to detect cleaved caspase-3 along with Hoechst 33258 dye.

Determination of *in vitro* ROS production. HC cells were seeded onto a 35-mm glass-based dish (2 × 10⁵ cells) and incubated at 37 °C with 5% CO₂ overnight. The next day, cells were co-incubated with different strains of fungi (5 × 10⁶ cells) for 8 hours. ROS production was analyzed based on the incorporation of CM-H2DCFDA (final concentration, 5 μM) (Life Technologies, Eugene, OR, USA) for 15 minutes at 37 °C, and cells were immediately monitored for their fluorescein isothiocyanate (FITC) fluorescence signals using confocal microscopy or an ImageXpress^{MICRO} High Content Screening System (Molecular Devices). The morphological analysis was performed using MetaXpress Image Analysis software (Molecular Devices).

Identification of ROS by ESR spectroscopy. Semi-quantitative measurements of the generated ROS were performed using a conventional spin trapping technique with ESR spectroscopy. Detailed methods are provided in the Supplemental Information. HC cells were seeded onto a 6-well plate (2 × 10⁵ cells) and incubated at 37 °C with 5% CO₂ overnight. Cells were co-incubated with the indicated fungi (5 × 10⁶ cells) for 8 hours. Culture media were diluted in 100 mM phosphate buffer (pH 7.4) containing 25 μM diethylenetriaminepentaacetic acid (DPTA) (Sigma-Aldrich Co.) and 25 mM BMPO (Enzo Life Sciences, Farmingdale, NY, USA)⁴⁰. The mixtures were then transferred to a quartz flat cell and set inside the cavity of the ESR spectrometer. Then, ESR measurements of the spin adducts were performed under the following conditions: magnetic field, 336.7 ± 10 mT; microwave frequency, 9.424 GHz; microwave power, 10.0 mW; sweep time, 0.5 minutes; time constant, 0.03 sec; and modulation field 1.0 × 0.1 mT (100 kHz). All ESR spectra were taken with 10 accumulation times. The generated ROS were evaluated using the data analyzer connected to the ESR spectrometer. Representative images obtained from a single experiment are shown.

***In vivo* fungal infection.** Six-week-old male C57BL/6/J mice, and 8-week-old female and male TG2^{+/+} and male TG2^{-/-} mice¹² were housed under constant temperature (22 °C ± 1 °C), with free access to food and water. To establish *in vivo* infection⁴¹, mice were injected via their lateral tail vein with approximately 4 × 10⁵, 4 × 10⁶, or 4 × 10⁷ cells/mouse of *C. albicans*. Mice were euthanized on the third or fourth day of infection after being anesthetized with isoflurane gas.

Determination of *in vivo* ROS production. Frozen liver tissue sections were washed twice with PBS and stained with 5 μM CM-H2DCFDA and incubated for 30 minutes at 37 °C. Subsequently, the tissue was washed twice with PBS and mounting medium, and cover slips were placed on the slides. The FITC fluorescence signals were detected using a Zeiss LSM 700 laser scanning confocal microscope.

Determination of *in vivo* TG activity. *In vivo* TG activity was assessed as previously reported^{42,43}. Briefly, 30 minutes prior to euthanasia, mice were injected with approximately 100 µg/g of 5-BAPA by intraperitoneal injection. Mice were then euthanized, and liver tissues were covered in optimal cutting temperature compound (OCT) and snap-frozen in liquid nitrogen. Sections (7 µm in thickness) were cut using a Leica sliding microtome (Leica Microsystems, Nussloch, Germany) and fixed in 4% paraformaldehyde. For histology, the sections were stained with Meyer's hematoxylin solution and 1% Eosin Y solution (Muto Pure Chemicals, Tokyo, Japan). For 5-BAPA staining, the sections were permeabilized with PBS/0.3% Triton X-100 and blocked with 5% goat serum in PBS at room temperature for 30 minutes. Thereafter, the sections were treated with streptavidin-TRITC (1:500 dilution, Jackson ImmunoResearch, West Grove, PA, USA) and Hoechst 33258 dye (1:5000 dilution, Wako Industries, Osaka, Japan) in blocking buffer at room temperature for 45 minutes. Immunofluorescence signals were detected using a Zeiss LSM 700 laser scanning confocal microscope.

Statistical analysis. Quantitative data are shown as the mean ± SD (n = 3–5). Statistical analyses were performed using GraphPad Prism version 6.0 for Windows (GraphPad Software, San Diego, CA, USA). A **p*-value < 0.05 and a ***p*-value < 0.01 were considered statistically significant.

References

- Kirpich, I. A. *et al.* Probiotics restore bowel flora and improve liver enzymes in human alcohol-induced liver injury: a pilot study. *Alcohol* **42**, 675–682 (2008).
- Zhu, L. *et al.* Characterization of gut microbiomes in nonalcoholic steatohepatitis (NASH) patients: a connection between endogenous alcohol and NASH. *Hepatology* **57**, 601–609 (2013).
- Llorente, C. & Schnabl, B. The gut microbiota and liver disease. *Cell Mol Gastroenterol Hepatol* **1**, 275–284 (2015).
- Mutlu, E. A. *et al.* Colonic microbiome is altered in alcoholism. *Am J Physiol Gastrointest Liver Physiol* **302**, G966–978 (2012).
- Yang, A. M. *et al.* Intestinal fungi contribute to development of alcoholic liver disease. *J Clin Invest* **63**, in press (2017).
- Brunke, S. & Hube, B. Two unlike cousins: *Candida albicans* and *C. glabrata* infection strategies. *Cell Microbiol.* **15**, 701–708 (2013).
- Perlroth, J., Choi, B. & Spellberg, B. Nosocomial fungal infections: epidemiology, diagnosis, and treatment. *Med Mycol* **45**, 321–346 (2007).
- Renna, M. S. *et al.* Hepatocellular apoptosis during *Candida albicans* colonization: involvement of TNF- α and infiltrating Fas-L positive lymphocytes. *Int Immunol* **18**, 1719–1728 (2006).
- Fleischhacker, M. *et al.* Diagnosis of chronic disseminated candidosis from liver biopsies by a novel PCR in patients with hematological malignancies. *Clin Microbiol Infect* **18**, 1010–1016 (2012).
- Nancy, R. *et al.* Fungal infection: a common, unrecognized complication of acute liver failure. *J Hepatol* **12**, 1–9 (1991).
- Fesus, L. & Szondi, Z. Transglutaminase 2 in the balance of cell death and survival. *FEBS Lett* **579**, 3297–3302 (2005).
- Tatsukawa, H. *et al.* Role of transglutaminase 2 in liver injury via cross-linking and silencing of transcription factor Sp1. *Gastroenterol.* **136**, 1783–1795 (2009).
- Kuo, T. F. *et al.* Free fatty acids induce transglutaminase 2-dependent apoptosis in hepatocytes via ER Stress-stimulated PERK pathways. *J. Cell. Physiol.* **227**, 1130–1137 (2012).
- Lee, Z. W. *et al.* Activation of *in situ* tissue transglutaminase by intracellular reactive oxygen species. *Biochem Biophys Res Commun.* **305**, 633–640 (2003).
- Yi, S. *et al.* Arachidonic acid activates tissue transglutaminase and stress fiber formation via intracellular reactive oxygen species. *Biochem Biophys Res Commun.* **325**, 819–826 (2004).
- Bhatt, M. P. *et al.* C-peptide prevents hyperglycemia-induced endothelial apoptosis through inhibition of reactive oxygen species-mediated transglutaminase 2 activation. *Diabetes* **62**, 243–253 (2013).
- Tatsukawa, H., Furutani, Y., Hitomi, K. & Kojima, S. Transglutaminase 2 has opposing roles in the regulation of cellular functions as well as cell growth and death. *Cell Death Dis* **7**, e2244 (2016).
- Yoo, J. O., Lim, Y. C., Kim, Y. M. & Ha, K. S. Transglutaminase 2 promotes both caspase-dependent and caspase-independent apoptotic cell death via the calpain/Bax protein signaling pathway. *The Journal of biological chemistry* **287**, 14377–14388 (2012).
- McConoughey, S. J. *et al.* Inhibition of transglutaminase 2 mitigates transcriptional dysregulation in models of Huntington disease. *EMBO Mol Med* **2**, 349–370 (2010).
- Martin, G., Rita, C. & Carlo, M. B. Transglutaminases: Nature's biological glue. *Biochem. J.* **368**, 377–396 (2002).
- Furutani, Y., Toguchi, M., Shrestha, R. & Kojima, S. Phenosafranin inhibits nuclear localization of transglutaminase 2 without affecting its transamidase activity. *Amino Acids*, doi:10.1007/s00726-016-2337-6 (2016).
- Koopman, W. *et al.* Simultaneous quantification of oxidative stress and cell spreading using 5-(and-6)-chloromethyl-2',7'-dichlorofluorescein. *Cytometry A* **69**, 1184–1192 (2006).
- Mark, R. *et al.* Yno1p/Aim14p, a NADPH-oxidase ortholog, controls extramitochondrial reactive oxygen species generation, apoptosis, and actin cable formation in yeast. *PNAS* **109**, 8658–8663 (2012).
- Sarmadi, B. H. & Ismail, A. Antioxidative peptides from food proteins: a review. *Peptides* **31**, 1949–1956 (2010).
- Schröter, C., Hipler, U. C., Wilmer, A., Künkel, W. & Wollina, U. Generation of reactive oxygen species by *Candida albicans* in relation to morphogenesis. *Arch Dermatol Res* **292**, 260–264 (2000).
- Stamnaes, J., Pinkas, D. M., Fleckenstein, B., Khosla, C. & Sollid, L. M. Redox regulation of transglutaminase 2 activity. *J Biol Chem* **285**, 25402–25409 (2010).
- Rolando, N., Philpott-Howard, J. & Williams, R. Bacterial and fungal infection in acute liver failure. *Liver Dis* **16**, 389–402 (1996).
- Naranjan, D., Rana, T. & Thomas, N. Role of oxidative stress in cardiovascular diseases. *J Hypertens* **18**, 655–673 (2000).
- Bin, Q. *et al.* A key role for the microglial NADPH oxidase in APP-dependent killing of neurons. *Neurobiol Aging* **27**, 1577–1587 (2006).
- Zhang, Y., Dawson, V. L. & Dawson, T. M. Oxidative stress and genetics in the pathogenesis of Parkinson's disease. *Neurobiol Dis* **7**, 240–250 (2000).
- Liao, D., Corle, C., Seagroves, T. N. & Johnson, R. S. Hypoxia-inducible factor-1 α is a key regulator of metastasis in a transgenic model of cancer initiation and progression. *Cancer Res* **67**, 563–572 (2007).
- David, C. S., Jimmy, L. K. & Charles, S. G. Roles of transglutaminases in cardiac and vascular diseases. *Front Biosci.* **12**, 2530–2545 (2009).
- Dean, M. H. *et al.* Transglutaminase induces protofibril-like amyloid β -protein assemblies that are protease-resistant and inhibit long-term potentiation. *J Biol Chem* **283**, 16790–16800 (2008).
- Bruce, A. C. *et al.* Protein crosslinking, tissue transglutaminase, alternative splicing and neurodegeneration. *Neurochem Int* **40**, 69–78 (2002).
- Bernassola, F. *et al.* Role of transglutaminase 2 in glucose tolerance: knockout mice studies and a putative mutation in a MODY patient. *FASEB J* **16**, 1371–1378 (2002).

36. Merve, E. *et al.* Up-regulation of TGM2 with ITGB1 and SDC4 is important in the development and metastasis of renal cell carcinoma. *Urol Oncol-Semin O* **125**, 25.e13–25.e20 (2014).
37. Fujise, K. *et al.* Integration of hepatitis B virus DNA into cells of six established human hepatocellular carcinoma cell lines. *Hepatology* **37**, 457–460 (1990).
38. Nanda, N. *et al.* Targeted inactivation of Gh/tissue transglutaminase II. *J Biol Chem* **276**, 20673–20678 (2001).
39. Akita, K. *et al.* Impaired Liver Regeneration in Mice by Lipopolysaccharide Via TNF- α /Kallikrein-Mediated Activation of Latent TGF- β . *Gastroenterol.* **123**, 352–364 (2002).
40. Zhao, H., Joseph, J., Zhang, H., Karoui, H. & Kalyanaraman, B. Synthesis and biochemical applications of a solid cyclic nitrene spin trap: a relatively superior trap for detecting superoxide anions and glutathyl radicals. *Free Radic. Biol. Med.* **31**, 599–606 (2001).
41. Vandeputte, P., Ischer, F., Sanglard, D. & Coste, A. T. *In vivo* systematic analysis of *Candida albicans* Zn2-Cys6 transcription factors mutants for mice organ colonization. *PLoS one* **6**, e26962 (2011).
42. DiRaimondo, T. R. *et al.* Elevated transglutaminase 2 activity is associated with hypoxia-induced experimental pulmonary hypertension in mice. *ACS Chem Biol* **9**, 266–275 (2014).
43. Dafik, L., Albertelli, M., Stamnaes, J., Sollid, L. M. & Khosla, C. Activation and inhibition of transglutaminase 2 in mice. *PLoS one* **7**, e30642 (2012).

Acknowledgements

This work was supported partly by Grant-in-Aids from the Ministry of Education, Science, Sports, and Culture and by a grant from the RIKEN CLST (No. 26102742 to SKo) and for the Research on the Innovative Development and the Practical Application of New Drugs for Hepatitis B (H24-B Drug Discovery Hepatitis General 003) from the AMED, Japan (for SKo). This work was also supported partly by grants from the National Key Research and Development Program of China (No. 2016YFD0400604 to MC), the National High Technology Research and Development Program of China (863 Program, No. 2013AA102205 to JL), and the General Program of National Natural Science Foundation of China (No. 31671963 to JL). RoS has been awarded the International Program Associate (IPA) fellowship from the RIKEN and Tokyo Institute of Technology, Japan. RaS has been awarded the International Program Associate (IPA) fellowship from the RIKEN and Tokyo Medical and Dental University, Japan. The funders had no role in study design, data collection and analysis, decision to publish, or preparation of the manuscript. The authors express sincere thanks to Prof. Reizo Kato (RIKEN, Japan) for his useful discussions as well as Prof. Robert M. Graham and Dr. Siiri E. Iismaa (Victor Chang Cardiac Research Institute, Australia) for providing TG2^{-/-} mice and useful discussion.

Author Contributions

S.Ka. and S.Ko. conceived and designed the experiments. Ro.S., Ra.S., X.Y.Q., Y.O., L.J., M.C., S. Ka. and S.Ko. drafted the manuscript. Ro.S., Ra.S., T.F.K., X.Y.Q., R.T., K.F., M.H., and M.L. collected the data and carried out the analysis with advice from Y.O., S.I., S.Ka. and S.Ko. A.N.T. and H.C. constructed the *NADPH* oxidase gene mutant of *C. glabrata* (*Cgnox1*). L.J. and M.C. prepared the corn peptide fractions. All authors were involved in the discussion and editing of the final manuscript.

Additional Information

Supplementary information accompanies this paper at doi:10.1038/s41598-017-04630-8

Competing Interests: The authors declare that they have no competing interests.

Publisher's note: Springer Nature remains neutral with regard to jurisdictional claims in published maps and institutional affiliations.



Open Access This article is licensed under a Creative Commons Attribution 4.0 International License, which permits use, sharing, adaptation, distribution and reproduction in any medium or format, as long as you give appropriate credit to the original author(s) and the source, provide a link to the Creative Commons license, and indicate if changes were made. The images or other third party material in this article are included in the article's Creative Commons license, unless indicated otherwise in a credit line to the material. If material is not included in the article's Creative Commons license and your intended use is not permitted by statutory regulation or exceeds the permitted use, you will need to obtain permission directly from the copyright holder. To view a copy of this license, visit <http://creativecommons.org/licenses/by/4.0/>.

© The Author(s) 2017